References

ALLPRESS, J. G. & SANDERS, J. V. (1973). *J. Appl. Cryst.* **6**, 165–190.

ALLPRESS, J. G., SANDERS, J. V. & WADSLEY, A. D. (1969). *Acta Cryst.* B**25**, 1156–1164.

BERTAUT, E. F. (1953). *Acta Cryst.* **6**, 557–561.

BUSECK, P. R. & IIJIMA, S. (1974). *Amer. Min.* **59**, 1–21.

COWLEY, J. M. & IIJIMA, S. (1972). *Z. Naturforsch.* **27**a, 445–451.

COWLEY, J. M. & MOODIE, A. F. (1957). *Acta Cryst.* **10**, 609–619.

DEVRIES, A. B. (1972). Dissertation, Univ. Groningen, Netherlands.

EISENHANDLER, C. B. & SIEGEL, B. M. (1966). *J. Appl. Phys.* **37**, 1613–1620.

FLEET, M. E. (1971). *Acta Cryst.* B**27**, 1864–1867.

GOODMAN, P. & LEHMPFUHL, G. (1967). *Acta Cryst.* **22**, 14–24.

GOODMAN, P. & MOODIE, A. F. (1974). *Acta Cryst.* A**30**, 280–290.

GRØNVOLD, F., HARALDSEN, H., PEDERSEN, B. & TUFTE, T. (1969). *Rev. Chim. Min.*, **6**, 215–240.

HEIDENREICH, R. D. (1964). In *Fundamentals of Transmission Electron Microscopy*, p. 165. New York: Interscience.

HORIUCHI, S. & MATSUI, Y. (1974). *Phil. Mag.* **30**, 777–787.

HORIUCHI, S., MATSUI, Y., KATO, K. & NAGATA, F. (1975). *Jap. J. Appl. Phys.* **14**, 1837–1838.

HORIUCHI, S., SAEKI, M., MATSUI, Y. & NAGATA, F. (1975). *Acta Cryst.* A**31**, 660–664.

IIJIMA, S. (1971). *J. Appl. Phys.* **49**, 5891–5893.

IIJIMA, S. (1973). *Acta Cryst.* A**29**, 18–24.

IIJIMA, S., KIMURA, S. & GOTO, M. (1973). *Acta Cryst.* A**29**, 632–636.

KAWADA, I., NAKANO-ONODA, M., ISHII, M., SAEKI, M., & NAKAHIRA, M. (1975). *J. Solid State Chem.* **15**, 246–252.

KOTO, K. (1976). To be published.

LYNCH, D. F., MOODIE, A. F. & O'KEEFE, M. A. (1975). *Acta Cryst.* A**31**, 300–307.

NAKANO-ONODA, M. & NAKAHIRA, M. (1976). To be published.

NAKAZAWA, H., MORIMOTO, N. & WATANABE, E. (1975). *Amer. Min.* **60**, 359–366.

NAKAZAWA, H., SAEKI, M. & NAKAHIRA, M. (1975). *J. Less-Common Met.* **40**, 57–63.

OKAZAKI, A. (1961). *J. Phys. Soc. Japan*, **16**, 1162–1170.

O'KEEFE, M. A. (1973). *Acta Cryst.* A**29**, 389–401.

PIERCE, L. & BUSECK, P. R. (1974). *Science*, **186**, 1209.

SAEKI, M. & NAKAHIRA, M. (1974). *J. Cryst. Growth*, **24/25**, 154–157.

SCHERZER, O. (1949). *J. Appl. Phys.* **20**, 20–29.

UYEDA, N., KOBAYASHI, T., SUITO, E., HARADA, Y. & WATANABE, M. (1972). *J. Appl. Phys.* **43**, 5181–5189.

Acta Cryst. (1976). A**32**, 565

Electron Population Analysis with Rigid Pseudoatoms

BY ROBERT F. STEWART*

Department of Chemistry, Carnegie-Mellon University, 4400 *Fifth Avenue, Pittsburgh, Pennsylvania*, 15213, *U.S.A.*

(*Received* 21 *July* 1975; *accepted* 30 *January* 1976)

The one-electron density function for a group of atoms within the asymmetric region of a unit cell is represented by a finite multipole expansion of the charge density about each atomic center. Each atomic expansion is called a pseudoatom. If the pseudoatom charge density is effectively rigid with nuclear motion, then the model may be used for a static charge density analysis of X-ray diffraction data. A valence density multipole model for pseudoatoms is restricted to single exponential radial functions. The representation is rotationally invariant. The model may be used for determination of static charge physical properties as well as aspects of chemical bonding. These results can be a critical test of the X-ray diffraction experiment for the determination of electron density distributions. The pseudoatoms discussed are primarily intended for crystals comprised of first and second-row atoms. The valence scattering model demands extensive data sets (probably at low temperatures) or an independent determination of atomic positions and mean square amplitudes of vibration.

Introduction

Over the last few years several models for a quantitative determination of electron density distributions from X-ray diffraction data have been proposed. Dawson (1967) proposed an atom deformation model which was extended by Kurki-Suonio (1968). Hirshfeld (1971) and Harel & Hirshfeld (1975) have applied the model to electron density analysis of organic molecular crystals. The model is a representation of the one-electron density function in the asymmetric part of the unit cell with a finite multipole expansion about the several atomic centers.

In the present paper several facets of the multipole model are reviewed within the framework of the fundamental theory for coherent X-ray scattering intensities. Several features of the model have been published in fragmentary reports by the author and by other workers. The effort here is an attempt to present the concept of pseudoatoms (or generalized X-ray

* Alfred P. Sloan Fellow.

scattering factors) in complete and unified form. Details of the pseudoatom model, which render intensity formulas tractable for electron density analysis, are developed for materials of low Z values (atoms with atomic number less than 18). A variety of static charge properties can be inferred from the model and compared to results from other experiments in chemical physics. Applications of the model to diffraction data and several restrictions are covered in the last sections of the paper.

Fundamental considerations

For an X-ray frequency far removed from an absorption frequency of a molecule, the intensity for coherent, elastic scattering is proportional to $|F|^2$ where

$$F(\mathbf{S},\mathbf{Q})=\int \varrho(\mathbf{r},\mathbf{Q}) \exp(i\mathbf{S}\cdot\mathbf{r})d\mathbf{r}\,. \quad (1)$$

Here $\mathbf{S}=2\pi(\mathbf{k}-\mathbf{k}_0)/\lambda$, where $\mathbf{k}$ and $\mathbf{k}_0$ are unit vectors in the direction of scattered and incident radiation, respectively. If the angle between $\mathbf{k}$ and $\mathbf{k}_0$ is 2θ, then $|\mathbf{S}|=4\pi \sin\theta/\lambda$. $\mathbf{S}$ is referred to as the Bragg vector. In (1), $\mathbf{Q}$ is a vector of all nuclear coordinates and $\varrho(\mathbf{r},\mathbf{Q})$ is the one-electron density function for the molecule (charge density function) at some $\mathbf{Q}$,

$$\varrho(\mathbf{r},\mathbf{Q})=\int \psi^*(\mathbf{r},s_1,\mathbf{x}_2,\ldots\mathbf{x}_N;\mathbf{Q}) \times \psi(\mathbf{r},s_1,\mathbf{x}_2,\ldots,\mathbf{x}_N;\mathbf{Q})d\mathbf{x}_N\ldots d\mathbf{x}_2 ds_1\,. \quad (2)$$

In (2), ψ is the wavefunction which solves the many-electron Schrödinger equation in the potential of fixed nuclei (it is an adiabatic wavefunction) and is spanned by both space and spin coordinates of each electron. Note that (2) is averaged over all electrons but one and includes an average over the spin of the last electron. It is important to point out that the amplitude of scattering from (1) is for a time scale $\sim 10^{-17}$–10^{-18} s. The basic theory for X-ray scattering on this time scale was reported by Waller & Hartree (1929) and is sufficiently accurate for further discussion. An understanding of the indistinguishability of electrons and the antisymmetric nature of ψ have come about since the Waller–Hartree theory, but these developments do not alter the basic validity of (1). The result, then, is that the short-time Bragg experiment is intimately related to the Fourier transform of a static charge density function and is a one-electron expectation value.

The actual observed intensity is on a long time scale (10^2–10^0 s) and is a statistical average over the states for $\mathbf{Q}$. In this case the canonical ensemble average for coherent scattering is,

$$I_{co}(\mathbf{S})=\frac{I_{cl}\int F^*(\mathbf{S},\mathbf{Q}')t(\mathbf{Q}'\mathbf{Q};\beta)F(\mathbf{S},\mathbf{Q})d\mathbf{Q}}{\int t(\mathbf{Q}',\mathbf{Q};\beta)d\mathbf{Q}}\,, \quad (\mathbf{Q}'=\mathbf{Q}) \quad (3)$$

where

$$t(\mathbf{Q}',\mathbf{Q};\beta)=\sum_n \varphi_n(\mathbf{Q}')\exp(-\beta H)\varphi_n(\mathbf{Q}) \quad (4)$$

is the Dirac density matrix. φ_n are state functions for the nuclei, $\beta=1/kT$, and H is the Hamiltonian for nuclear motion. In (3) I_{cl} is the classical scattering of unpolarized light by an electron at a distance r from the observer as given by Thomson & Thomson (1933),

$$I_{cl}=\tfrac{1}{2}(e^2/rmc^2)^2(1+\cos^2 2\theta)^2. \quad (5)$$

The extension of $\varrho(\mathbf{r},\mathbf{Q})$ from (2) to a giant molecule or small crystal lattice does not introduce anything fundamentally new to the theory. The dimensions of $\mathbf{Q}$ are dramatically increased and translational symmetry comes into consideration. Equation (3) is an essentially correct theory of coherent X-ray scattering. The results above are taken from Born (1942–1943).

The diffracted X-ray intensities from real crystals suffer absorption and some interaction between incident and scattered radiation within the crystal. It will be assumed in this work that kinematic diffraction theory is applicable. Developments by Zachariasen (1967) and Becker & Coppens (1974) lend credence to the presumption that observed X-ray diffraction intensities for many crystals can be reduced to the moduli of kinematic structure factors. However, $|F_{kin}|^2$ is *not* simply related to (3) by absorption, the volume of the crystal and a Lorentz factor. Born's (1942–1943) result for scattering by a molecule in equation (3) includes *inelastic*, coherent scattering, which in a crystal lattice is known as thermal diffuse scattering. For this case $\mathbf{k}$ differs from $\mathbf{k}_0$ by the momentum of a phonon or vibron, which is small compared to $\mathbf{k}_0$. An explicit decomposition of (3) into 'atomic' densities is given below with the aim of relating (3) to kinematic structure factors.

Pseudoatoms in molecules and crystals

In order to render (3) tractable for a crystallographic structure analysis, several approximations are usually made. One starts with $I_{co}(\mathbf{S},\mathbf{Q})$ [*i.e.* $F^*(\mathbf{S},\mathbf{Q})F(\mathbf{S},\mathbf{Q})$ with $F(\mathbf{S},\mathbf{Q})$ from (1)] as an expansion about $\mathbf{Q}_e$, the equilibrium nuclear configuration. If the nuclei move in a potential that is dominant in displacements from $\mathbf{Q}_e$ that are quadratic, then the motion of the nuclei is amenable to a normal coordinate analysis and it is easy to solve for $t(\mathbf{Q},\mathbf{Q};\beta)$. The harmonic oscillator approximation alone, however, does not render equation (3) tractable for structure analysis. The charge density function in the asymmetric part of a unit cell can be decomposed as a superposition of pseudoatom charge densities centered about each nucleus. The second assumption is that the pseudoatoms are rigid in that they perfectly follow the motion of the nuclei upon which they are respectively centered.

The harmonic motion and rigid pseudoatom approximations result in an explicit form for (3) as given by

Born (1942–1943),

$$I_{co}(\mathbf{S}) \simeq \sum_{p,p'} F_p^* F_{p'} \prod_j \exp\left[-\tfrac{1}{2}(\mu_{pp'}^j)\bar{\varepsilon}_j \omega_j^{-2}\right] \quad (6)$$

where $\bar{\varepsilon}_j$ is the thermal mean energy of a harmonic oscillator with angular frequency ω_j and the product over j covers the N normal modes in the crystal lattice. $F_p(\mathbf{S})$ can be written as

$$F_p(\mathbf{S}) = f_p(\mathbf{S}) \exp(i\mathbf{S} \cdot \mathbf{R}_p) \quad (7)$$

where $\mathbf{R}_p$ is a three-component vector of nucleus p for $\mathbf{Q} = \mathbf{Q}_e$ and $f_p(\mathbf{S})$ is the Fourier transform of the rigid pseudoatom about nucleus p. Note that *rigid* means that $f_p(\mathbf{S})$ is not a function of $\mathbf{Q}$. The other term in (6) is

$$(\mu_{pp'}^j)^2 = |\mathbf{S}|^2 \left[\frac{(e_{pq}^j)^2}{M_p} + \frac{(e_{p'q}^j)^2}{M_{p'}} - \frac{2e_{pq}^j e_{p'q}^j}{\sqrt{M_p M_{p'}}}\right] \quad (8)$$

where e_{pq}^j is the component of $e_p^j/\sqrt{M_p}$, the amplitude vector of nucleus p with mass M_p for the vibration j, along the direction of $\mathbf{S}$. The first two terms on the right-hand side of (8) give rise to the Bragg diffraction of rigid pseudoatoms that are uncorrelated in their motion and the third term, which represents correlation of the nuclear motion, gives rise to thermal diffuse scattering. In this paper it will be assumed that an appropriate correction can be made. With the long-range order of a real crystal the phonon–photon momentum exchange can preserve sufficient coherence to participate in the Bragg diffracted intensities. Borie (1970), among others, gives a rather good account of this phenomenon. Approximate corrections of X-ray diffraction data for thermal diffuse scattering are possible (see for example Lucas, 1969). By neglecting or correcting for the cross term in (8), (6) can be factored into a structure factor equation where the components for the tensor of the mean square motions of nucleus p, $\mathbf{U}_p$, are

$$U_{p,\alpha\beta} = M_p^{-1} \sum_j \bar{\varepsilon}_j e_{p\alpha}^j e_{p\beta}^j / \omega_j^2 \quad \alpha,\beta = x,y,z\,. \quad (9)$$

Up to now, the pseudoatom or its Fourier transform, $f_p(\mathbf{S})$, has not been specified. Debye (1930) suggested that the pseudoatom be represented as an isolated atom. In the absence of fields external to the nucleus (a massive point charge) and the electrons the atomic charge density is necessarily spherically symmetrical. In this case $f_p(\mathbf{S})$ is $f_p(S)$, that is, the atomic scattering factor only depends on the magnitude of the Bragg vector but not on its direction. One need not be so restrictive in the representation of $\varrho(\mathbf{r},\mathbf{Q})$ from (2) as a superposition of isolated atoms. It is possible to represent each pseudoatom as a finite multipole expansion in the mean square sense and to determine the radial pseudoatom density functions from a known $\varrho(\mathbf{r},\mathbf{Q})$. For such an expansion the molecular expectation values of several one-electron operators are correctly given. A general formalism for diatomic molecules has been reported (Stewart, Bentley & Goodman, 1975) and detailed examples for first-row atom systems have been given (Bentley & Stewart, 1975). In this work it is proved that the expectation, $\langle g(r_a)P_j(\cos\theta_a)\rangle$, is correctly given for $j \leq J$, where J is the largest multipole expansion on center a, regardless of the expansion on center b, and $g(r_a)$ is an arbitrary function of r_a (scalar) for which the integral exists. Extension to polyatomic systems is apparently straightforward but at this juncture the author cannot establish uniqueness in the solution to the least-squares equations. The main point, however, is that $\varrho(\mathbf{r},\mathbf{Q})$ can be represented by a small, multipole expansion about each nuclear center to rather high accuracy. The rigidity of such pseudoatoms remains to be studied and can be explored with a study of accurate charge density functions at several values of $\mathbf{Q}$.

If we assume that Bragg diffraction intensities can be properly corrected for thermal diffuse scattering, then we must yet be properly concerned with anharmonic motion of the nuclei as well as deformation of the pseudoatoms. Low-frequency and acoustical modes in the lattice have good size anharmonic components, but in this case the pseudoatoms are only marginally deformed (*e.g.* rigid-body motion of molecules in molecular crystals). On the other hand, high-frequency modes such as bond stretches in molecular crystals are rather localized and can lead to sizable deformations of pseudoatom charge density functions. Librational motions, such as oscillations of methyl groups, are both anharmonic and deforming. The magnitude of these effects on Bragg intensities in X-ray diffraction needs to be determined. In any event, any serious development beyond the harmonic oscillator approximation for the motion of nuclei must also include the dependence of pseudoatoms or generalized X-ray scattering factors on the positions of the nuclei. The development below is a model based on the rigid-pseudoatom and harmonic-motion approximations for the analysis of X-ray diffraction data for charge density information.

Restricted radial density basis functions

The representation of the one-electron density function (2) as a superposition of rigid pseudoatoms should conform to several ground rules. The expansion must be rotationally invariant and the density function must obey classical laws of electrostatics. It is desirable, though not necessary, to use quantum chemical experience in the choice of bases to span the pseudoatom on center p.

Let the nuclear coordinates, $\mathbf{Q}_e$, be at equilibrium and define the row vector $\mathbf{Q}_e^t$ as $(\mathbf{R}_1^t, \mathbf{R}_2^t, \ldots \mathbf{R}_p^t, \ldots \mathbf{R}_N^t)$ where $\mathbf{R}_p^t$ is (x_p, y_p, z_p) for nucleus p of the N nuclei in the asymmetric part of the unit cell. The charge density function for the electrons is a finite multipole expansion

$$\varrho(\mathbf{r},\mathbf{Q}_e) = \sum_{p=1}^{N} \sum_{l=0}^{L} \left[\sum_{m=0}^{l} C_{plm}^e B_{plm}^e(\mathbf{r}-\mathbf{R}_p) + \sum_{m=1}^{l} C_{plm}^o B_{plm}^o(\mathbf{r}-\mathbf{R}_p)\right] \quad (10)$$

where C^e_{plm} and C^o_{plm} are electron population coefficients. The basis functions B^e_{plm} and B^o_{plm} are

$$B^e_{plm}(\mathbf{r}_p)=(4\pi)^{-1}R_{pl}(\mathbf{r}_p)P^m_l(\cos\theta_p)\cos m\varphi_p$$
$$B^o_{plm}(\mathbf{r}_p)=(4\pi)^{-1}R_{pl}(\mathbf{r}_p)P^m_l(\cos\theta_p)\sin m\varphi_p \quad (11)$$

where $R_{pl}(r_p)$ is a radial function for the lth-order multipole of pseudoatom p and $P^m_l(\cos\theta_p)$ is an associated Lengendre function. Since the tesseral harmonics $P^m_l(\cos\theta)\begin{Bmatrix}\cos m\varphi\\ \sin m\varphi\end{Bmatrix}$ form a basis for the irreducible representation of the full rotation group, the expansion (10) is rotationally invariant and therefore independent of the choice of coordinate system. The radial functions for the pseudoatom, however, still need to be specified.

In the formation of chemical bonds the charge density near the nucleus of the atom is largely unaffected by the rest of the atomic environment. We shall assume that each pseudoatom (except hydrogen) has a 'core' invariant part and a deformable valence part. The core density function, therefore, will have a fixed electron population. The valence radial functions are approximated by single exponential type functions. Thus,

$$R_{p,0}(r_p)=2\chi^2_{1s}(r_p)+C_{p,0}r_p^{npo}\exp(-\alpha_p r_p)$$

and

$$R_{p,l}(r_p)=r_p^{npl}\exp(-\alpha_p r_p), \quad l\geq 1. \quad (12)$$

In (12) $\chi_{1s}(r_p)$ is a normalized $1s$ spin restricted atomic orbital for the solution of the Hartree–Fock equations of motion for an isolated atom. For the valence radial functions, $n_{pl}\geq l$ to ensure a proper solution of Poisson's equation at $r_p=0$ for a Coulomb potential. The 'size' of the valence radial function is determined by α_p as well as n_{pl}. Quantum chemical estimates for the exponential parameter ($\alpha_p=2\zeta_p$) for the first-row atoms have been reported by Hehre, Stewart & Pople (1969). The α_p, however, can be made a variable parameter in the analysis of X-ray diffraction data (*cf.* Stewart, 1973*b*).

Several examples of the basis functions (11) and (12) are displayed in Figs. 1 to 6 where α_p (3·90 bohr^{-1}) is for a standard molecular nitrogen atom (Hehre, Stewart & Pople, 1969). The contours are in arbitrary units of electrons (bohr)$^{-3}$; the box is 5 bohr or 2·65 Å on each side.

Extensive studies of single exponential radial functions as bases for mean-square fits to one-electron density functions of diatomic molecules have been carried out by Bentley (1975). Several molecular averages are approximately ($\sim$10%) reproduced by the superposition of the pseudoatoms given in (12). Results of this work will be reported in a sequel to the present paper. The restricted radials proposed here are probably sufficient for an approximate static charge density model in the analysis of X-ray diffraction data.

The Fourier transform of (11) is a basis for the representation of $f_p(\mathbf{S})$ in (7). The generalized X-ray scattering factor [the Fourier transform of (11)] is,

$$f^e_{plm}(\mathbf{S})=i^l f_{pl}(S)P^m_l(\eta_s)\cos m\varphi_s$$
$$f^o_{plm}(\mathbf{S})=i^l f_{pl}(S)P^m_l(\eta_s)\sin m\varphi_s \quad (13)$$

where $i=\sqrt{-1}$, $\eta_s=\cos\theta_s$ and φ_s are the angular components of the Bragg vector, and

$$f_{pl}(S)=\int_0^\infty R_{p,l}(r_p)j_l(sr_p)r_p^2\,dr_p \quad (14)$$

where $j_l(x)$ is an lth-order spherical Bessel function. The pseudoatom on center p, therefore, has the Fourier

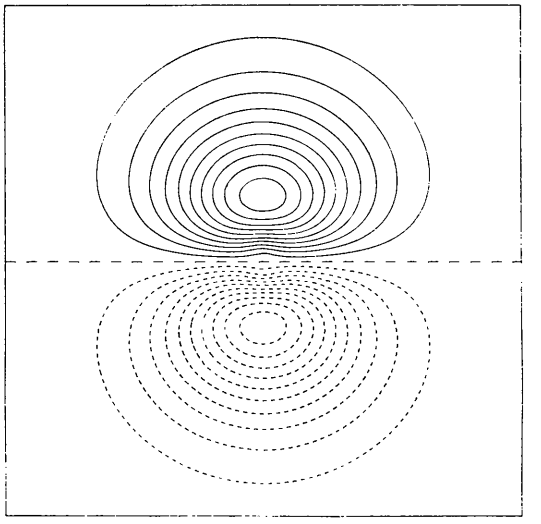

Fig. 1. Electron density plot of $xr\exp(-\alpha r)$ at $z=0$. $\alpha=3{\cdot}9$ bohr^{-1}. ——— Positive density in steps of 10. — — — zero density. ----- negative density in steps of -10. Contours are proportional to electrons bohr^{-3}.

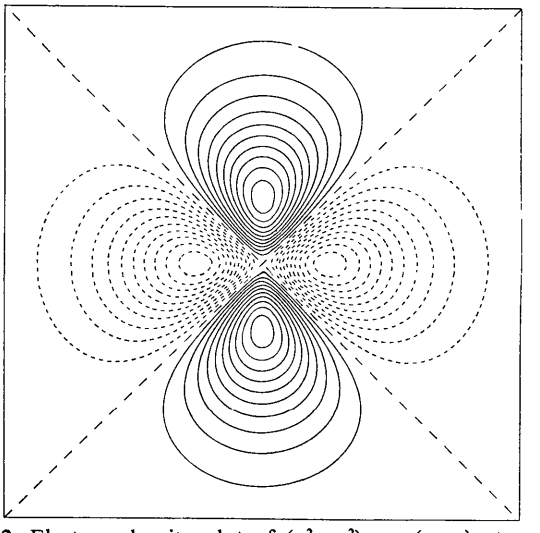

Fig. 2. Electron density plot of $(x^2-y^2)\exp(-\alpha r)$ at $z=0$. $\alpha=3{\cdot}9$ bohr^{-1}. Contours are proportional to electrons bohr^{-3}. Solid and dashed lines are the same as for Fig. 1.

transform,

$$f_p(\mathbf{S}) = \sum_{l=0}^{L} \left[\sum_{m=0}^{l} C^e_{plm} f^e_{plm}(\mathbf{S}) + \sum_{m=1}^{l} C^o_{plm} f^o_{plm}(\mathbf{S}) \right] . \quad (15)$$

Equations (14) and (15) can serve as a basis for electron population analysis of X-ray data. The valence model discussed below is restricted in that (12) is used for an evaluation of (14).

Least-squares applications

It need not be assumed that absolute structure factors are available. It will be assumed that an X-ray data set of structure factor moduli are proportional to an absolute set of $|F_{hkl}|$ with one scale factor. Extension to several data sets is not difficult. For atom p let

$$E(\mathbf{x}_p, \beta_p) = \exp(2\pi i \mathbf{H}^t \mathbf{x}_p) \exp(-\mathbf{H}^t \beta_p \mathbf{H}) \quad (16)$$

where $\mathbf{x}_p$ is the time average nuclear position, $\mathbf{H}$ is the Bragg vector with components in Miller indices and β_p

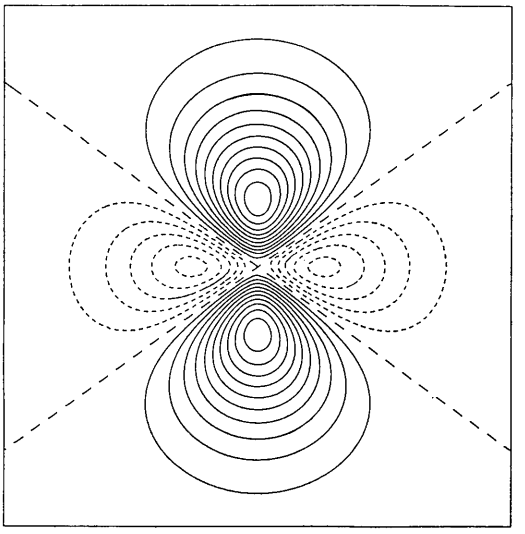

Fig. 3. Electron density plot of $[z^2-(\frac{1}{5})r^2] \exp(-\alpha r)$ at $x=0$. $\alpha=3{\cdot}9$ bohr^{-1}. Contours are proportional to electrons bohr^{-3}. Solid and dashed lines are the same as for Fig. 1.

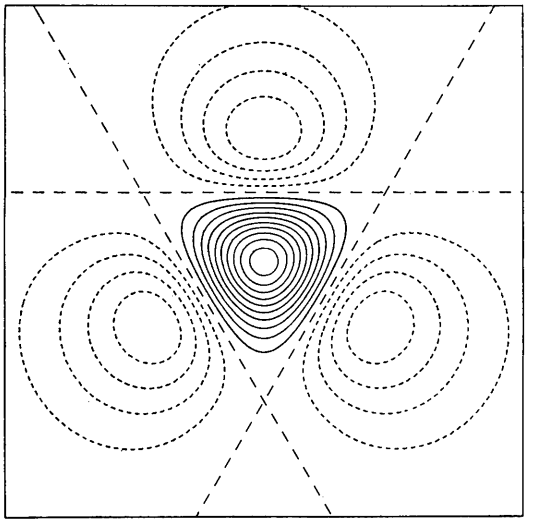

Fig. 5. Electron density plot of $xyz \exp(-\alpha r)$ in the plane $x+y+z=3\sqrt{3}/\alpha$, $\alpha=3{\cdot}9$ bohr^{-1}. This plane is 0·705 Å from the origin. Contours are proportional to electrons bohr^{-3}. Solid and dashed lines are the same as for Fig. 1.

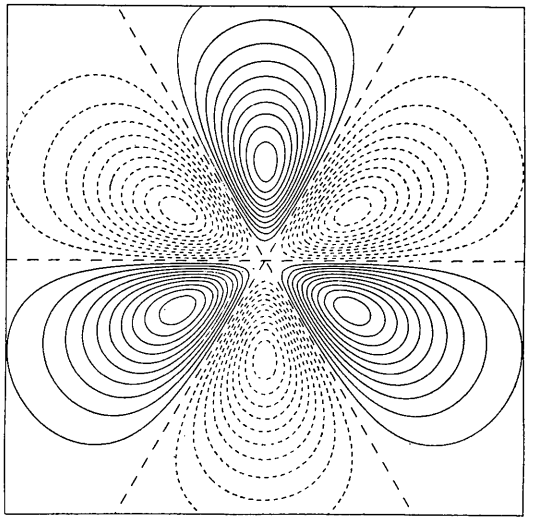

Fig. 4. Electron density plot of $(x^2-3y^2)x \exp(-\alpha r)$ at $z=0$. $\alpha=3{\cdot}9$ bohr^{-1}. Contours are proportional to electrons bohr^{-3}. Solid and dashed lines are the same as for Fig. 1.

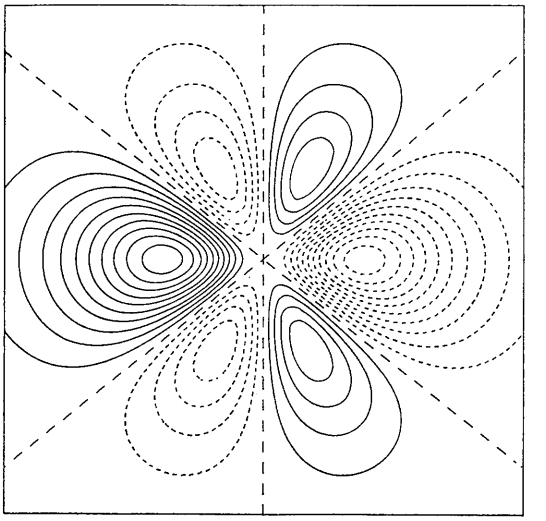

Fig. 6. Electron density plot of $(5z^2-3)z \exp(-\alpha r)$ at $x=0$. $\alpha=3{\cdot}9$ bohr^{-1}. Contours are proportional to electrons bohr^{-3}. Solid and dashed lines are the same as for Fig. 1.

is the tensor for vibrational motion. The structure factor model is,

$$F_c(\mathbf{H}) = \sum_{\text{sym}} \sum_p f_p(\mathbf{C},\mathbf{H}) E(\mathbf{x}_p, \beta_p) \qquad (17)$$

where $\mathbf{C}$, $\mathbf{x}_p$ and β_p are parameters in the model. Note that if $\mathbf{x}_p$ is the equilibrium position for atom p then (17) is a factor in (6). The sum over p is for the asymmetric unit and the sum over 'sym' extends over the symmetry operations in the unit cell. The vector array $\mathbf{C}$ in f_p needs to be specified.

The core part of f_p is held invariant to electron population analysis and, for a first-row atom, is

$$f_{\text{core}}(H) = 2\int_0^\infty R_{\text{core}}(r) j_0(Sr) r^2 \mathrm{d}r \qquad (18)$$

where $R_{\text{core}}(r) = 4\pi\chi_{1s}^2$ and χ_{1s} is the SCF $1s$ orbital of the first-row atom. For the evaluation of (18) $S = 2\pi a_0(\mathbf{H}^t\mathbf{M}\mathbf{H})^{1/2}$ with $a_0 = 0{\cdot}529177$ Å and $\mathbf{M}$ is the metric tensor of the crystal. A possible extension is to add the anomalous dispersion terms $\Delta f'$ and $i\Delta f''$ to (18). The remaining terms in $f_p(\mathbf{C},\mathbf{H})$ may be assigned variable electron population parameters and comprise the valence scattering model. Thus, one may write

$$\begin{aligned} f_p(\mathbf{C},\mathbf{H}) = {} & k f_{\text{core}}(H) + C_{p0} f_{p0}(H) \\ & + i f_{p1}(H)[C_{p11} P_1^1(\cos\theta_H)\cos\varphi_H \\ & + C_{p12} P_1^1(\cos\theta_H)\sin\varphi_H + C_{p13} P_1^0(\cos\theta_H)] \\ & - f_{p2}(H)[C_{p21} P_2^2(\cos\theta_H)\cos 2\varphi_H \\ & + C_{p22} P_2^2(\cos\theta_H)\sin 2\varphi_H \\ & + C_{p23} P_2^1(\cos\theta_H)\cos\varphi_H \\ & + C_{p24} P_2^1(\cos\theta_H)\sin\varphi_H \\ & + C_{p25} P_2^0(\cos\theta_H)] + \ldots \quad . \end{aligned} \qquad (19)$$

The factor k in (19) is the usual overall scale factor. The angular functions $[P_l^m(\cos\theta_H)\cos m\varphi_H$ and $P_l^m(\cos\theta_H)\sin m\varphi_H]$ for the Bragg vector must transform as the symmetry operations in the unit cell. For example, the odd orders (dipole and octupole functions), which are purely imaginary, must be combined with the sine terms of $E(\mathbf{x}_p, \beta_p)$ in (16) for centrosymmetric structures. A systematic way to apply these functions to charge density analyses is to take them in groups of their order. For an atom that has a site symmetry of 1, all three P_1^m and/or all five P_2^m and/or all seven P_3^m must be included to ensure rotational invariance.

For computational work it is more convenient to use a Cartesian representation of the tesseral harmonics in the expansion (19). A summary of these multipole basis functions up through fourth order is given in Table 1. [Octupole and hexadecapole bases were reported by Stewart (1973*a*), but are included here for convenience.] The site symmetry of the atom may force several components in (19) to have zero population. Symmetry constraints for dipoles and quadrupoles are given in Tables 2 and 3 respectively. Tabulations for third and fourth-order terms have been given by Stewart (1973*a*). Note that the dipole terms are apropos of pseudoatoms in a low site symmetry. For organic molecular crystals, where often the approximate site symmetry is high, one can anticipate rather small con-

Table 1. *Multipole basis functions*

The q_x, q_y, q_z are direction cosines of the Bragg vector in an arbitrary orthogonal coordinate system. The P_l^m are unnormalized associated Legendre functions.

$f(q_x,q_y,q_z)$	Tesseral harmonic	$f(q_x,q_y,q_z)$	Tesseral harmonic
q_x	$P_1^1\cos\varphi$	$q_x^2-q_y^2$	$(\frac{1}{3})P_2^2\cos 2\varphi$
q_y	$P_1^1\sin\varphi$	q_xq_y	$(\frac{1}{6})P_2^2\sin 2\varphi$
q_z	P_1^0	q_xq_z	$(\frac{1}{3})P_2^1\cos\varphi$
$q_x^4-6q_x^2q_y^2+q_y^4$	$(\frac{1}{105})P_4^4\cos 4\varphi$	q_yq_z	$(\frac{1}{3})P_1^1\sin\varphi$
$(q_x^2-q_y^2)q_xq_y$	$(\frac{1}{420})P_4^4\sin 4\varphi$	$q_z^2-\frac{1}{3}$	$(\frac{2}{3})P_2^0$
$(q_x^2-3q_y^2)q_xq_z$	$(\frac{1}{105})P_4^3\cos 3\varphi$	$(q_x^2-3q_y^2)q_x$	$(\frac{1}{15})P_3^3\cos 3\varphi$
$(3q_x^2-q_y^2)q_yq_z$	$(\frac{1}{105})P_4^3\sin 3\varphi$	$(3q_x^2-q_y^2)q_y$	$(\frac{1}{15})P_3^3\sin 3\varphi$
$(7q_z^2-1)(q_x^2-q_y^2)$	$(\frac{2}{15})P_4^2\cos 2\varphi$	$(q_x^2-q_y^2)q_z$	$(\frac{1}{15})P_3^2\cos 2\varphi$
$(7q_z^2-1)q_xq_y$	$(\frac{1}{15})P_4^2\sin 2\varphi$	$q_xq_yq_z$	$(\frac{1}{30})P_3^2\sin 2\varphi$
$(7q_z^2-3)q_xq_z$	$(\frac{2}{5})P_4^1\cos\varphi$	$(5q_z^2-1)q_x$	$(\frac{2}{3})P_3^1\cos\varphi$
$(7q_z^2-3)q_yq_z$	$(\frac{2}{5})P_4^1\sin\varphi$	$(5q_z^2-1)q_y$	$(\frac{2}{3})P_3^1\sin\varphi$
$7q_z^4-6q_z^2+\frac{3}{5}$	$(\frac{8}{5})P_4^0$	$(5q_z^2-3)q_z$	$2P_3^0$

Table 2. *Non-vanishing atomic dipole components for site symmetries*

The z axis is along the direction of maximum symmetry.

	Site symmetry			
Components	1	m	2, 3, 4, 6 $3m$, $4/m$ $6mm$, $mm2$	All other crystallographic point groups
q_x	C_{p11}	C_{p11}	0	0
q_y	C_{p12}	C_{p12}	0	0
q_z	C_{p13}	0	C_{p13}	0

Table 3. *Non-vanishing atomic quadrupole components for site symmetries*

The z axis is along the direction of maximum symmetry.

	Site symmetry				
Components	$\frac{1}{\bar{1}}$	2 m $2/m$	222 mmm $mm2$	$\bar{3}$, $\bar{3}m$, 3, $3m$, 32 4, $4mm$, $\bar{4}$, $4/m$, 422 $\bar{4}2m$, $4/mmm$, 6, $6mm$ $\bar{6}$, $6/m$, 622, $\bar{6}m2$, $6/mmm$	All other crystallographic point groups
$q_x^2-q_y^2$	C_{p21}	C_{p21}	C_{p21}	0	0
q_xq_y	C_{p22}	C_{p22}	0	0	0
q_xq_z	C_{p23}	0	0	0	0
q_yq_z	C_{p24}	0	0	0	0
$q_z^2-\frac{1}{3}$	C_{p25}	C_{p25}	C_{p25}	C_{p25}	0

tributions of the three dipole components to the valence charge density of the pseudoatoms. Quadrupole deformation functions may play a more prominent role. For carbon atoms, octupole deformation functions are probably most suitable for a valence charge density analysis.

The C_{plm} are electron population parameters to be determined by the method of least squares. The relative magnitudes of C_{plm} determine the orientation of a particular multipole for the pseudoatom. For example, an aromatic carbon atom has an approximate site symmetry of $\bar{6}m2$. One would expect the dipole terms to have negligible population, one dominant quadrupole and one dominant octupole component. To establish this with the diffraction data one must include all three dipole functions in the analysis. If the magnitudes of C_{plm} are small (of the order of the estimated standard deviation), they can properly be neglected. Analysis for the quadrupole deformation must include all five functions and for third-order tesserals all seven must be included. The final orientations of the octupole and quadrupole moments of the pseudoatoms are key factors in a critical appraisal of the diffraction data for valence charge information. One way to visualize the final results is to construct an electron density map of the pseudoatom multipole(s) of interest. Stereo plots of these deformation functions for 2,4,6-triamino-*s*-triazine (Larson & Cromer, 1974) and for 1,1′-azobiscarbamide (Cromer & Larson, 1974) have been published. One can also rotate the results into a local coordinate system. For the example of an aromatic C atom one anticipates a single dominant quadrupole and octupole term. Let $\mathbf{b}_l$ be Cartesian basis functions of tesserals in the coordinate system for the least-squares analysis and let $\mathbf{b}'_l$ be the set in the local coordinate system. Then,

$$\mathbf{b}'_l = \mathscr{R}_l \mathbf{b}_l \tag{20}$$

where $\mathscr{R}_l$ is a matrix of order $(2l+1)$ and is explicitly given by Cromer, Larson & Stewart (1976). If $\mathbf{C}_{pl}$ is the vector of population coefficients from the least-squares result,

$$\mathbf{C}^t_{pl}\mathbf{b}_l = \varrho_{pl}(\mathbf{r}_p) = \mathbf{C}^{t'}_{pl}\mathbf{b}'_l \tag{21}$$

where $\mathbf{C}'_{pl}$ is the column vector of population coefficients in the local coordinate system. [The notation of superscript t is the transpose, or in the case of (21) a row vector.] From (20) and (21) it follows,

$$\mathbf{C}'_{pl} = [\mathscr{R}_l^{-1}]^t \mathbf{C}_{pl} \,. \tag{22}$$

Equation (22) can be a valuable aid in the interpretation of electron population results from X-ray diffraction data.

The radial distribution scattering factors (14) can be analytically evaluated when the restricted radial functions (12) are used. An explicit form useful for computation can be found in Watson (1966). The radial scattering factors when weighted by S^2, generally show maxima at larger sin θ/λ with increasing order of the tesseral harmonic. One such family of curves for a P atom was published by Stewart (1973*a*). This general feature by rather different radial scattering functions has been noted by Kurki-Suonio (1968). For valence-shell radial density functions of first-row atoms most of the radial scattering is within an Ewald sphere of 0·8 Å^{-1} in sin θ/λ and the functions have maxima typically in the range 0·3–0·5 Å^{-1} in sin θ/λ.

It is also possible and desirable to refine on the single exponential parameter, α_p in (12). In the normal equations for least squares, then,

$$\partial f_p(S,\alpha_p)/\partial\alpha_p = -\int_0^\infty r_p^{npl+3} \exp(-\alpha_p r_p) j_l(Sr_p) \mathrm{d}r_p \tag{23}$$

where (23) follows from (14) and (12) by straightforward differentiation of (14). Equation (23) is of the same family of hypergeometric functions as (14) and is computationally tractable.

Interpretation of results

The rigid pseudoatom model can be used to determine a number of one-electron molecular averages. Such physical properties are excellent criteria for a critical evaluation of the results. All such evaluations involve integration of a spatial operator and the density basis functions (11) over all space. The single exponential radial functions in (12) are not normalized. This is convenient for least-squares analysis in reciprocal space, particularly when the exponential parameter, α_p, is being refined. For the evaluation of molecular averages, however, it is convenient to convert the final C_{plm} parameters into more direct electron population parameters with the normalization factor of the radial functions (12),

$$P_{plm} = [(n_{pl}+2)!/(\alpha_p)^{npl+3}] C_{plm} \,. \tag{24}$$

The P_{plm} are electron population parameters that one would get from the least-squares analysis had normalized radial valence functions been used. For absolute structure factors, the P_{p00} are just the total charge of the valence electrons on the several p atoms in the cell. If a scale factor is varied in least squares in addition to C_{plm}, then P_{p00}/k is the valence charge for atom p where k is the structure-factor scale factor. (As discussed below k only multiplies atoms or parts of atoms with fixed electron populations.) One critical test of the valence monopole density functions, then, is to see how closely the P_{p00}/k sum to the total valence charge. Cromer & Larson (1974) and Larson & Cromer (1974) find agreement to within several percent. The elimination of k for a constrained refinement is given below in the section on practical applications.

The evaluation of other physical properties such as dipole moments and electric field gradients with the present model has been outlined by Stewart (1972). The expectations of irregular spherical harmonics, such as electric fields and field gradients, only included con-

tributions from local pseudoatoms. The contributions of neighboring pseudoatoms to field gradients are not negligible, however. The relevant penetration integrals for the potential, electric field, and electric field gradient from the bases (11) and (12) can be easily derived from the work of Pitzer, Kern & Lipscomb (1962). These expressions and the ones reported by Stewart (1972) can be used to estimate a variety of static charge properties from the valence structure analysis of the X-ray data. Comparison of electric field gradients with an NQR experimental result is desirable. In this case the orientation of the field gradient from the X-ray analysis ought to agree with the NQR result, unless the atom has a very large r.m.s. amplitude of motion. The principal axis components and asymmetry parameter determined by NQR may differ greatly from the X-ray result since the resonance experiment is sensitive to the environment in the immediate neighborhood of the nucleus, whereas X-ray diffraction data generally cannot resolve fine details of charge density in regions $\lesssim 0{\cdot}01$ Å from the nucleus.

Hydrogen atoms

A rigid pseudoatom model for terminally bonded hydrogen atoms is difficult to apply to X-ray diffraction data. A single monopole is rather inflexible and cannot adequately represent the true charge deformation near the proton. Although a single monopole scattering factor for H atoms gave chemically reasonable charges in earlier work (Stewart, 1970), it undoubtedly does not refine to the time-average proton position. The absence of a core structure for hydrogen atoms is the limiting feature. Determination of the proton position and simultaneously the dipole deformation terms from X-ray data alone is not feasible. An independent determination of the time-average proton position or of the charge anisotropy is necessary. If the H atom charge is polarized along the covalent bond towards the heavier atom, a cylindrically symmetric model for the H pseudoatom is perhaps reasonable. Dipole deformation scattering factors for terminally bonded H atoms can be extracted from model systems for which accurate wavefunctions exist. It would be of interest to see if such functions would promote refinement of the H atom onto the time-average proton position. But the electron population analysis would still be restricted to a single monopole function. If the proton position and mean square amplitude of vibration were determined from neutron diffraction data, then one could use the X-ray data for analysis of several multipole population parameters for the pseudoatoms of hydrogen. For the present a rather limited scattering model for bonded hydrogens is recommended by employing a single monopole scattering factor. In previous work Stewart (1972) pointed out that inaccuracy of the proton position from refinement of X-ray diffraction data can be a severe limitation in the determination of physical properties by X-ray diffraction.

Practical considerations

The valence electron scattering model discussed above can be used in an X-ray structure analysis under several conditions. In (19) k is the scale factor and is to multiply any scattering factor for which a fixed electron population is assumed. If the C_{plm} from (15) are set to zero for $l \geq 1$ and the C_{p00} are fixed so that P_{p00} from (24) are the neutral atomic valence electron number, then (17) is the standard structure factor model that is widely used in crystal structure analysis.

Suppose E from (16) has been determined from neutron diffraction data and it is desired to use this information in (17). The parameters sought from the X-ray data are the scale factor k, and the electron population parameters C_{plm}. In this case the least-squares problem is linear in the parameter space. One may also choose to constrain the valence monopole population coefficients to sum to the product of the scale factor and total number of valence electrons. This constraint eliminates one of the linear parameters in the least-squares problem. It is convenient to eliminate the scale factor by

$$k = \sum_{\text{sym}} \sum_{p} P_{p00}/F_v(000) \tag{25}$$

where P_{p00} is given in (24) and $F_v(000)$ is the total number of valence electrons in the unit cell. With the constraint (25), the normal equations from minimization with respect to C_{p00} will have the factors

$$\partial F_c/\partial C_{p00} = \sum_{\text{sym}} [N_p(n_p, \alpha_p) f_{p,0}(H) + \sum_{q} N_q n_p, \alpha_p) f_{\text{core},q}/F\,(000)] E(\mathbf{x}_p, \beta_p)$$

and

$$N_p(n_p, \alpha_p) = (n_{p0}+2)!/\alpha_p^{np0+3}\,. \tag{26}$$

If the valence density monopole functions are relatively efficient in accounting for the total valence charge, then (25) and (26) should not severely alter the results from an unconstrained least-squares treatment. If it is also desired to refine the exponential parameters with the constraint (25) then minimization with respect to α_p leads to the factor,

$$\partial F_c/\partial \alpha_p = \sum_{\text{sym}} [C_{p00}(N'_p f_{p0} + N_p f'_{p0}) + \sum_{q} C_{q00} N'_p f_{\text{core},q}/F_v(000)] E(\mathbf{x}_p, \beta_p)$$

$$N'_p = -(n_{p0}+3)!/(\alpha_p)^{np0+4} \tag{27}$$

and f'_{p0} is given by (23).

A further extension of the pseudoatom density model may be desired if $E(\mathbf{x}_p, \beta_p)$ is also to be determined from X-ray diffraction data. Since the radial scattering factors for the several valence multipoles can extend out to $\sim 0{\cdot}8$ Å^{-1} in $\sin\theta/\lambda$, an extensive data set is needed. With inclusion of dipole terms, a correlation problem is introduced. The partial derivative of F_c with respect to a positional parameter generates a scattering function which is approximately proportion-

al to $f_{p,1}(H)$ for sin θ/λ up to 0·6 Å^{-1}. A weaker, but similar correlation occurs between thermal parameters and $f_{p,2}(H)$. To estimate the correlation factor of a dipole coefficient with a positional parameter, the following sums have been evaluated:

$$a_1=\sum_x x^2 f_{p,1}^2 \exp(-16\pi^2 U x^2),$$
$$a_2=\sum_x x^2 f_{p,1} f_N \exp(-16\pi^2 U x^2), \qquad (28)$$
$$a_3=\sum_x x^2 f_N^2 \exp(-16\pi^2 U x^2),$$

where f_N is the total scattering factor for a nitrogen atom, $f_{p,1}$ is the radial dipole scattering factor for the valence shell of N, x is sin θ/λ and U is the mean square amplitude of vibration of the atom. For a monatomic crystal, the estimated correlation coefficient,

$$C(x_{\max}, U)=-a_2/\sqrt{a_1 a_3}. \qquad (29)$$

The estimates are listed in Table 4 as a function of maximum sin θ/λ and of U. In order for the magnitude of the correlation coefficients to be less than 0·7, one sees that the model is very demanding on the size of the data set. The small correlation coefficients with smaller temperature factors further indicate that the valence model is more useful at low temperatures if one desires to determine both atomic positions and dipole population coefficients with nearly independent precision estimates.

The estimated correlation coefficients between a pseudoatom quadrupole moment and a thermal parameter are tabulated in Table 5. The same expression (29) was used, but $f_{p,2}$ was substituted for $f_{p,1}$ in (28). The trend is similar to, but decidedly less than the results in Table 4. For small U values, however, the estimated correlation is comparable to the dipole case. Correlation between the parameters of $E(\mathbf{x}_p, \beta_p)$ and population coefficients for octupole or higher-order poles is considerably smaller than the examples given here.

These estimated correlation coefficients can provide some guidance in the use of the pseudoatom model for a charge density analysis of X-ray diffraction data. For example, with a set of Cu $K\bar{\alpha}$ diffraction data and no independent determination of atomic positions and amplitudes of vibration, it would be pointless to extend the valence model beyond a monopole population analysis. For a very extensive data set [(sin $\theta/\lambda)_{\max} > 0{\cdot}8$ Å^{-1}] one might anticipate an improvement in the accuracy of both atomic positions and thermal parameters. The valence scattering model has sufficient flexibility to accommodate much of the atomic charge deformation, reflected by the medium-order data, whereby the atomic positions and thermal parameters will have greater freedom to describe the nuclear properties of the molecular crystal. It is the high-order data which give the most accurate information on both the time-average nuclear positions and the mean square displacements of the atom. The reason for this is that the

Table 4. *Estimated correlation coefficient between atomic position parameter and pseudoatom dipole parameter as a function of mean square amplitude motion and data set size*

	(sin $\theta/\lambda)_{\max}$ (Å^{-1})							
U ($\times 10^2$ Å^2)	0·65	0·80	0·90	1·0	1·1	1·2	1·3	1·4
0·63	−0·839	−0·717	−0·629	−0·573	−0·514	−0·479	−0·445	−0·420
1·27	−0·850	−0·746	−0·676	−0·635	−0·596	−0·575	−0·557	−0·546
1·90	−0·860	−0·776	−0·724	−0·697	−0·673	−0·663	−0·655	−0·651
2·53	−0·873	−0·806	−0·770	−0·753	−0·740	−0·735	−0·733	−0·732
3·17	−0·885	−0·834	−0·810	−0·800	−0·794	−0·792	−0·791	
3·80	−0·897	−0·859	−0·843	−0·838	−0·835	−0·835		
4·43	−0·909	−0·880	−0·871	−0·868	−0·867			
5·07	−0·919	−0·899	−0·899	−0·892				
5·70	−0·928	−0·914	−0·911	−0·911				
6·33	−0·937	−0·927	−0·925					

Table 5. *Estimated correlation coefficient between atomic thermal parameters and pseudoatom quadrupole parameter as a function of mean square amplitude motion and data set size*

	(sin $\theta/\lambda)_{\max}$ (Å^{-1})							
U ($\times 10^2$ Å^2)	0·65	0·80	0·90	1·0	1·1	1·2	1·3	1·4
0·63	−0·873	−0·760	−0·670	−0·608	−0·537	−0·493	−0·445	−0·408
1·27	−0·873	−0·763	−0·679	−0·625	−0·566	−0·533	−0·500	−0·479
1·90	−0·874	−0·772	−0·698	−0·654	−0·610	−0·589	−0·570	−0·560
2·53	−0·877	−0·784	−0·723	−0·690	−0·661	−0·649	−0·640	−0·636
3·17	−0·882	−0·800	−0·752	−0·729	−0·711	−0·705	−0·702	−0·700
3·80	−0·887	−0·818	−0·782	−0·767	−0·757	−0·754	−0·753	
4·43	−0·894	−0·836	−0·811	−0·802	−0·797	−0·796		
5·07	−0·901	−0·855	−0·837	−0·832	−0·830	−0·829		
5·70	−0·908	−0·872	−0·861	−0·858	−0·857			
6·33	−0·915	−0·888	−0·881	−0·879				

core electron structure of the atom at large sin θ/λ makes the X-ray analysis become similar to the neutron diffraction model.

Another possible application of the valence scattering model is a joint refinement of X-ray and neutron data where $\mathbf{x}_p$ and β_p are taken as common to the two experimental results. Coppens (1971) has suggested such an approach with a 'double atom' model for the static charge density of a molecular crystal. In this model an L-shell monopole scattering factor is allowed to float off the core scattering position. For small shifts ($\sim$0·01 Å), the floated L-shell density function is essentially a small multipole expansion about the core scattering position. From an economical point of view of the fewest least-squares parameters for the best density representation, the double atom refinement may be preferable to the more formal model outlined here.

It is important to recall that the amplitude of coherent X-ray scattering by a unit cell is decomposed into a sum of generalized X-ray scattering factors. If the scattering about one center is poorly represented, then a least-squares analysis for nearby pseudoatoms may lead to non-local behavior even though these centers are well spanned by the generalized X-ray scattering factors. An example is the present model of a single monopole for H atom scattering. Population coefficients for the quadrupole and/or octupole scattering factors centered on the atom to which the hydrogen is bonded, are forced to accommodate some of the polarized electron density about the proton. Such a delocalized pseudoatom is probably far from rigid in its response to nuclear motion so that the basic deconvolution approximation may seriously break down. In this case, the electron population parameters cannot be expected to give reliable static-charge physical properties of the crystal system.

Conclusion

The valence scattering model is based on a multipole expansion similar to the proposal of Kurki-Suonio (1968). The radial functions, however, are restricted to single exponential functions. The multipole expansion on the several centers is a rotationally invariant representation of the static-charge density function and can efficiently span charge in chemical bonds. Application of the present model to electron population analysis demands extensive X-ray diffraction data, preferably low-temperature results, or an independent determination of atomic positions and thermal parameters. The proposed electron density basis functions can be used to determine a variety of electrostatic physical properties which serve as criteria for a critical evaluation of charge density results from X-ray diffraction data.

Generous support by the Alfred P. Sloan Foundation is much appreciated. This research was supported by the National Science Foundation Grant MPS74-17592.

References

BECKER, P. J. & COPPENS, P. (1974). *Acta Cryst.* A**30**, 129–147.
BENTLEY, J. J. (1975). Ph. D. Thesis, Carnegie-Mellon Univ.
BENTLEY, J. J. & STEWART, R. F. (1975). *J. Chem. Phys.* **63**, 3794–3803.
BORIE, B. (1970). *Acta Cryst.* A**26**, 533–535.
BORN, M. (1942–1943). *Rep. Progr. Phys.* **9**, 294–333.
COPPENS, P. (1971). *Acta Cryst.* B**27**, 1931–1938.
CROMER, D. T. & LARSON, A. C. (1974). *J. Chem. Phys.* **60**, 176–184.
CROMER, D. T., LARSON, A. C. & STEWART, R. F. (1976). *J. Chem. Phys.* Submitted.
DAWSON, B. (1967). *Proc. Roy. Soc.* A**298**, 255–263.
DEBYE, P. (1930). *Phys. Z.* **31**, 419–428.
HAREL, M. & HIRSHFELD, F. L. (1975). *Acta Cryst.* B**31**, 162–172.
HEHRE, W. J., STEWART, R. F. & POPLE, J. A. (1969). *J. Chem. Phys.* **51**, 2657–2664.
HIRSHFELD, F. L. (1971). *Acta Cryst.* B**27**, 769–781.
KURKI-SUONIO, K. (1968). *Acta Cryst.* A**24**, 379–390.
LARSON, A. C. & CROMER, D. T. (1974). *J. Chem. Phys.* **60**, 185–192.
LUCAS, B. W. (1969). *Acta Cryst.* A**25**, 627–631.
PITZER, R. M., KERN, C. W. & LIPSCOMB, W. N. (1962). *J. Chem. Phys.* **37**, 267–274.
STEWART, R. F. (1970). *J. Chem. Phys.* **53**, 205–213.
STEWART, R. F. (1972). *J. Chem. Phys.* **57**, 1664–1668.
STEWART, R. F. (1973*a*). *J. Chem. Phys.* **58**, 1668–1676.
STEWART, R. F. (1973*b*). *J. Chem. Phys.* **58**, 4430–4438.
STEWART, R. F., BENTLEY, J. J. & GOODMAN, B. (1975). *J. Chem. Phys.* **63**, 3786–3793.
THOMSON, J. J. & THOMSON, G. P. (1933). *Conduction of Electricity Through Gasses*, 3rd ed. Vol. II, pp. 257–260. Cambridge Univ. Press.
WALLER, I. & HARTREE, D. R. (1929). *Proc. Roy. Soc.* A**124**, 119–142.
WATSON, G. N. (1966). *A Treatise on the Theory of Bessel Functions*, p. 385. Cambridge Univ. Press.
ZACHARIASEN, W. H. (1967). *Acta Cryst.* **23**, 558–564.